



HAL
open science

On the controlled evolution of level sets and like methods: the shape and contrast reconstruction

Christophe Ramananjaona, Marc Lambert, Dominique Lesselier, Jean-Paul Zolesio

► To cite this version:

Christophe Ramananjaona, Marc Lambert, Dominique Lesselier, Jean-Paul Zolesio. On the controlled evolution of level sets and like methods: the shape and contrast reconstruction. A. Wirgin. Acoustics, Mechanics, and the Related Topics of Mathematical Analysis - Proceedings of the International Conference to Celebrate Robert P Gilbert's 70th Birthday, World Scientific; WORLD SCIENTIFIC, pp.243-250, 2003, 9789812382641; 9789812704405. 10.1142/9789812704405_0036 . hal-00638240

HAL Id: hal-00638240

<https://hal.science/hal-00638240>

Submitted on 26 Jan 2024

HAL is a multi-disciplinary open access archive for the deposit and dissemination of scientific research documents, whether they are published or not. The documents may come from teaching and research institutions in France or abroad, or from public or private research centers.

L'archive ouverte pluridisciplinaire **HAL**, est destinée au dépôt et à la diffusion de documents scientifiques de niveau recherche, publiés ou non, émanant des établissements d'enseignement et de recherche français ou étrangers, des laboratoires publics ou privés.

ON THE CONTROLLED EVOLUTION OF LEVEL SETS AND LIKE METHODS: THE SHAPE AND CONTRAST RECONSTRUCTION

C. RAMANANJAONA, M. LAMBERT AND D. LESSELIER

*Département de Recherche en Électromagnétisme,
Laboratoire des Signaux et Systèmes,
3, rue Joliot-Curie, Plateau de Moulon, 91192 Gif-sur-Yvette cedex, France
E-mail: christophe.ramananjaona@lss.supelec.fr, marc.lambert@lss.supelec.fr,
dominique.lesselier@lss.supelec.fr*

J.-P. ZOLÉSIO

*INRIA
2004, route des Lucioles, B.P. 93,
06902 Sophia-Antipolis cedex, France
E-mail: jean-paul.zolesio@sophia.inria.fr*

The controlled evolution of level sets provides a successful framework to solve time-harmonic inverse scattering problems for objects whose contrast with the environment is known but whose shape is unknown³. New solution tools extend this framework to the retrieval of objects whose both shape and contrast are unknown.

1. A short introduction to the level set technique

The level set representation of domains enables to describe the evolution of fronts¹, and is now used in a variety of applications², including inverse scattering problems^{3,4,5,6}. The idea of using level sets to retrieve location and shape of an unknown homogeneous and penetrable object embedded in a portion (some search domain D) of a known space by the observation of the scattered field on a set of receivers M which is resulting from its interaction with an impinging time-harmonic pressure wave lies in the combination of two techniques:

- (i) the representation of a bounded domain Ω (singly- or multiply-connected as well) within D by a function Φ whose zero-levels correspond to the boundary contours $\partial\Omega$;
- (ii) the speed method, which consists in the construction of a velocity field ensuring a deformation of Ω , a properly chosen objective or cost

functional J being minimized ⁷.

Like with many inverse problems, the solution is obtained by iterative minimization of J , the latter measuring the discrepancy between the field u_S scattered by Ω and data ζ collected by the sensors at the frequency(ies) ω of operation for probing field(s) u_I . The scattering problem itself is approached via a (scalar) contrast-source domain integral formulation and the application of a method of moments at the discretization stage ⁸. The formulation is similar to the one developed earlier in the TM-polarization case in 2-D electromagnetics ^{3,5}. State (coupling) and observation (data) equations respectively read as

$$u(\vec{x}) = u_I(\vec{x}) + k_0^2 \int_{\Omega} \eta G_{oo}(\vec{x}, \vec{y}) u(\vec{y}) d\vec{y}, \quad \forall \vec{x} \in D, \quad (1)$$

$$u_S(\vec{x}) = k_0^2 \int_{\Omega} \eta G_{or}(\vec{x}, \vec{y}) u(\vec{y}) d\vec{y}, \quad \forall \vec{x} \in M. \quad (2)$$

In the above Green functions G_{or} and G_{oo} with source point \vec{y} and observation point \vec{x} are used, index o standing for a point in the search domain D and index r for a point in the measurement domain M ; the wave number of the host medium D is $k_0(\omega)$, and the scatterer is of wave number $k(\omega)$; contrast η reads as $\eta = \frac{k^2(\omega)}{k_0^2(\omega)} - 1 = \frac{c_0^2}{c^2} - 1$, where c_0 and c are the velocities of the pressure wave inside the host medium and the scatterer, respectively, both media being fluid and with unit density.

When the contrast η is known, the problem comes down to an optimal shape design problem in some pseudo-time t (in the discrete model, the number of iterations), with the associated objective functional

$$J(\Omega) = \frac{1}{2} \|u_S(\Omega) - \zeta\|_{L^2(M)}^2. \quad (3)$$

The gradient of J with respect to the variation of shape is handled via a Lagrangian formulation ⁵, and reads as

$$\frac{dJ}{dt} = \Re \mathbf{e} \left(k_0^2 \int_{\partial\Omega} \eta u(\vec{s}) p(\vec{s}) \vec{V}(\vec{s}) \cdot \vec{n}(\vec{s}) d\vec{s} \right), \quad (4)$$

where u is the total field in D ; p the adjoint field, computed as usual by assuming that the measurement set M radiates an incident field of complex-valued amplitude $\overline{u_S(\Omega) - \zeta}$, the overbar denoting complex-conjugation; \vec{n} the normal to the boundary contour $\partial\Omega$ (assumed regular enough); and \vec{V} the speed of evolution of this boundary. The choice of

$$\vec{V} = -\Re \mathbf{e} (k_0^2 \eta u p) \vec{n} \quad (5)$$

along $\partial\Omega$ provides in theory a strictly negative derivative of J . Upon extending the above speed to the whole of D , the motion of every level of Φ —the level 0 is $\partial\Omega$ —is described by the Hamilton-Jacobi equation ¹,

$$\frac{d\Phi}{dt}(\vec{x}) + \vec{V}(\vec{x}) \cdot \vec{n}(\vec{x}) \|\vec{\nabla}\Phi(\vec{x})\| = 0, \forall \vec{x} \in D. \quad (6)$$

Examples of such reconstructions are available in different electromagnetic and acoustic configurations ^{5,9}.

2. Shape and contrast reconstruction

The simultaneous retrieval of contrast η and shape Ω is a demanding task. Variations of the cost functional (3) now read as

$$dJ = \frac{\partial J}{\partial \chi} d\chi + \frac{\partial J}{\partial \eta} d\eta \quad (7)$$

where χ is the support of Ω . The partial derivation of J with respect to χ is dealt with as is usual within the level set method (4). As for the partial derivation of J with respect to η , it can be performed either in full, which means the variations of the total field vs. η are accounted for in the calculation, or in approximate fashion, which means the total field u is kept constant in the estimation. (Details of the calculations are given next.)

Once suitable derivatives in the direction of η and χ are available, an alternating procedure can be built: shape contours are updated by the level set method until convergence, then contrasts are updated by an optimization algorithm adapted to non-linear problems (such as the Levenberg-Marquardt method ¹⁰) until convergence, and the procedure is repeated from the new updates until a satisfactory solution is obtained.

The full calculation of the derivative with respect to the contrast proceeds as follows. The cost functional (3) is cast into a constrained Lagrangian:

$$J = \min_{w \in H^1(\Omega)} \max_{\phi \in H^1(\Omega)} \mathcal{L},$$

$$\mathcal{L}(w, \bar{w}, \phi, \bar{\phi}) = \frac{1}{2} \int_M \left| \int_{\Omega} \eta G_{or}(\vec{x}, \vec{y}) w(\vec{y}) d\vec{y} - \zeta(\vec{x}) \right|^2 d\vec{x}$$

$$+ \Re \int_{\Omega} \left(w(\vec{x}) - u_I(\vec{x}) - \int_{\Omega} \eta G_{oo}(\vec{x}, \vec{y}) w(\vec{y}) d\vec{y} \right) \phi(\vec{x}) d\vec{x}, \quad (8)$$

the saddle-point $(u, \bar{u}, \psi, \bar{\psi})$ of which is verified to be unique ⁵ by considering the change of variable, $\forall \vec{x} \in \Omega$,

$$\psi(\vec{x}) = -k_0^2 \eta p(\vec{x}). \quad (9)$$

Then, application of Cuer-Zolésio's theorem ¹¹ yields the derivative of J as

$$\frac{\partial J}{\partial \eta} = \frac{\partial \mathcal{L}}{\partial \eta}(u, \bar{u}, \psi, \bar{\psi}). \quad (10)$$

Now, in order to use the Levenberg-Marquardt algorithm, the complex-valued contrast is written as $\eta(a, b) = a + ib$, and the derivations are performed with respect to the real-valued coefficients a and b .

By derivating (8) with respect to a , one obtains

$$\begin{aligned} \frac{\partial J}{\partial a}(a, b) &= \int_M \left\{ a \left| k_0^2 \int_{\Omega} G_{or}(\bar{x}, \bar{y}) u(\bar{y}) d\bar{y} \right|^2 \right. \\ &\quad \left. - \Re \left(\overline{k_0^2 \zeta(\bar{x})} \int_{\Omega} \overline{G_{or}(\bar{x}, \bar{y}) u(\bar{y})} d\bar{y} \right) \right\} d\bar{x} \\ &\quad - \Re \int_{\Omega} k_0^2 \int_{\Omega} G_{oo}(\bar{x}, \bar{y}) u(\bar{y}) d\bar{y} \psi(\bar{x}) d\bar{x}; \end{aligned} \quad (11)$$

Noticing that $\forall z_1, z_2 \in \mathbb{C}$, $\Re(z_1 \bar{z}_2) = \Re(\bar{z}_1 z_2)$, Eq. (11) is rewritten as

$$\begin{aligned} \frac{\partial J}{\partial a}(a, b) &= \Re \int_M \bar{\eta} \left[k_0^2 \int_{\Omega} G_{or}(\bar{x}, \bar{y}) u(\bar{y}) d\bar{y} \right] \left[\overline{k_0^2 \int_{\Omega} G_{or}(\bar{x}, \bar{y}) u(\bar{y}) d\bar{y}} \right] d\bar{x} \\ &\quad - \Re \int_M k_0^2 \overline{\zeta(\bar{x})} \int_{\Omega} G_{or}(\bar{x}, \bar{y}) u(\bar{y}) d\bar{y} d\bar{x} \\ &\quad - \Re \int_{\Omega} k_0^2 \int_{\Omega} G_{oo}(\bar{x}, \bar{y}) u(\bar{y}) d\bar{y} \psi(\bar{x}) d\bar{x}. \end{aligned} \quad (12)$$

Performing the change of variable defined in (9), applying Fubini's theorem, and using Eq. (2), one gets

$$\begin{aligned} \frac{\partial J}{\partial a}(a, b) &= \Re \int_{\Omega} \bar{\eta} k_0^2 u(\bar{y}) \int_M G_{ro}(\bar{y}, \bar{x}) \overline{k_0^2} \int_{\Omega} \overline{G_{or}(\bar{x}, \bar{z}) u(\bar{z})} d\bar{z} d\bar{x} d\bar{y} \\ &\quad - \Re \int_{\Omega} u(\bar{y}) k_0^2 \int_M G_{ro}(\bar{y}, \bar{x}) \overline{\zeta(\bar{x})} d\bar{x} d\bar{y} \\ &\quad + \Re \int_{\Omega} k_0^2 u(\bar{y}) k_0^2 \eta \int_{\Omega} G_{oo}(\bar{x}, \bar{y}) p(\bar{x}) d\bar{x} d\bar{y}. \end{aligned} \quad (13)$$

This gives, using the reciprocity relation of the Green functions,

$$\begin{aligned} \frac{\partial J}{\partial a}(a, b) &= \Re \int_{\Omega} u(\bar{y}) k_0^2 \left[\int_M G_{or}(\bar{x}, \bar{y}) (\overline{u_S(\bar{x})} - \zeta(\bar{x})) d\bar{x} \right. \\ &\quad \left. + k_0^2 \int_{\Omega} G_{oo}(\bar{x}, \bar{y}) \eta p(\bar{x}) d\bar{x} \right] d\bar{y}, \end{aligned} \quad (14)$$

and finally, by definition of p ,

$$\frac{\partial J}{\partial a}(a, b) = \Re \left[k_0^2 \int_{\Omega} u(\bar{x}) p(\bar{x}) d\bar{x} \right]. \quad (15)$$

The derivation with respect to b can be carried out rather similarly: starting with

$$\begin{aligned} \frac{\partial J}{\partial b}(a, b) &= \int_M \left\{ b \left| k_0^2 \int_{\Omega} G_{or}(\vec{x}, \vec{y}) u(\vec{y}) d\vec{y} \right|^2 \right. \\ &\quad \left. - \Im \left(\overline{k_0^2 \zeta(\vec{x})} \int_{\Omega} \overline{G_{or}(\vec{x}, \vec{y}) u(\vec{y})} d\vec{y} \right) \right\} \\ &\quad + \Im \int_{\Omega} k_0^2 \int_{\Omega} G_{oo}(\vec{x}, \vec{y}) u(\vec{y}) d\vec{y} \psi(\vec{x}) d\vec{x}, \end{aligned} \quad (16)$$

using the property $\forall z_1, z_2 \in \mathbb{C}$, $\Im(z_1 \bar{z}_2) = -\Im(\bar{z}_1 z_2)$, and the same properties as those used for $\frac{\partial J}{\partial a}$, one finally gets

$$\frac{\partial J}{\partial b}(a, b) = -\Im \left[k_0^2 \int_{\Omega} u(\vec{x}) p(\vec{x}) d\vec{x} \right]. \quad (17)$$

The use of such derivatives requires the availability of the total field u and of its adjoint p at each iteration step of the η -optimization procedure, and this might become computationally costly. A less computationally demanding calculation of an approximated derivative is as follows. Derivating the cost functional (3), u being taken as a constant, yields

$$\begin{aligned} \frac{\partial J}{\partial a} \Big|_u(a, b) &= \int_M \left\{ a \left| k_0^2 \int_{\Omega} G_{or}(\vec{x}, \vec{y}) u(\vec{y}) d\vec{y} \right|^2 \right. \\ &\quad \left. - \Re \left(\overline{k_0^2 \zeta(\vec{x})} \int_{\Omega} \overline{G_{or}(\vec{x}, \vec{y}) u(\vec{y})} d\vec{y} \right) \right\} d\vec{x}, \end{aligned} \quad (18)$$

$$\begin{aligned} \frac{\partial J}{\partial b} \Big|_u(a, b) &= \int_M \left\{ b \left| k_0^2 \int_{\Omega} G_{or}(\vec{x}, \vec{y}) u(\vec{y}) d\vec{y} \right|^2 \right. \\ &\quad \left. - \Im \left(\overline{k_0^2 \zeta(\vec{x})} \int_{\Omega} \overline{G_{or}(\vec{x}, \vec{y}) u(\vec{y})} d\vec{y} \right) \right\} d\vec{x}. \end{aligned} \quad (19)$$

Let us notice that the approximated derivatives are similar to the exact ones in Eq. (11) and Eq. (16), the last terms taken out.

For each of those expressions, one could have obtained it directly by calculating $\frac{\partial J}{\partial \eta}$ ¹², which enables to write, for the full derivative,

$$\frac{\partial J}{\partial \eta} = \frac{1}{2} \left(\frac{\partial J}{\partial a} - i \frac{\partial J}{\partial b} \right) = \frac{k_0^2}{2} \int_{\Omega} u(\vec{x}) p(\vec{x}) d\vec{x}, \quad (20)$$

and for the approximated derivative,

$$\begin{aligned} \frac{\partial J}{\partial \eta} \Big|_u &= \frac{1}{2} \int_M \left[\bar{\eta} \left| k_0^2 \int_{\Omega} G_{or}(\vec{x}, \vec{y}) u(\vec{y}) d\vec{y} \right|^2 \right. \\ &\quad \left. - k_0^2 \bar{\zeta}(\vec{x}) \int_{\Omega} G_{or}(\vec{x}, \vec{y}) u(\vec{y}) d\vec{y} \right] d\vec{x}. \end{aligned} \quad (21)$$

3. Numerical examples

Using proper derivatives (4), (15), (17), (18) and (19), various algorithms can be devised by choosing the order and the accuracy of each optimization procedure⁹. Requiring a minimal value of the cost functional separately in the search of shape η and in the one of contrast χ , and alternating one search of each kind is the option taken from now.

For simplicity, only the case of lossless media will be considered, which means that only the derivative with respect to a is considered. Let us consider for example the configuration sketched in Table 1.

Table 1.

Incident waves	36 line sources, in circle, radius 3 mm
Frequencies	500, 1000, 1500, 2000 kHz
Receivers	64, on a circle of radius 2.5 mm
Domain D	$2 \times 2 \text{ mm}^2$, $c_0 = 1470 \text{ m.s}^{-1}$
Defect	2 rectangles, $c = 1800 \text{ m.s}^{-1}$

The scatterer domain is initialized as a centered disc the radius of which is equal to one-fourth of the side of the search domain, the first guess of its acoustic velocity being 1600 m.s^{-1} . Figure 1 displays the evolution of the cost functional J (here, the sum of the costs at all observation frequencies) and of the retrieved velocity c of the scatterer as a function of the number of iterations; the correspondingly retrieved domains are displayed in Figure 2.

One observes that the approximated calculation of the derivative yields a correct solution (the two rectangles) after not too high a number of iterations (with a cost functional reaching its least magnitude at iteration 41), but this result is not stable, since the procedure diverges beyond (at iteration 100 the velocity is unrealistically huge and the two rectangles are reduced almost to point scatterers ...). In contrast, with the full calculation of the derivative, the retrieved domains stay almost the same beyond the iteration at which the minimum of the cost functional is reached (at iteration 39), being said that the velocity fluctuates somewhat around the true value. Notice that both methods however provide the same velocity (about $c = 1770 \text{ m.s}^{-1}$) at the minimum of the cost functionals.

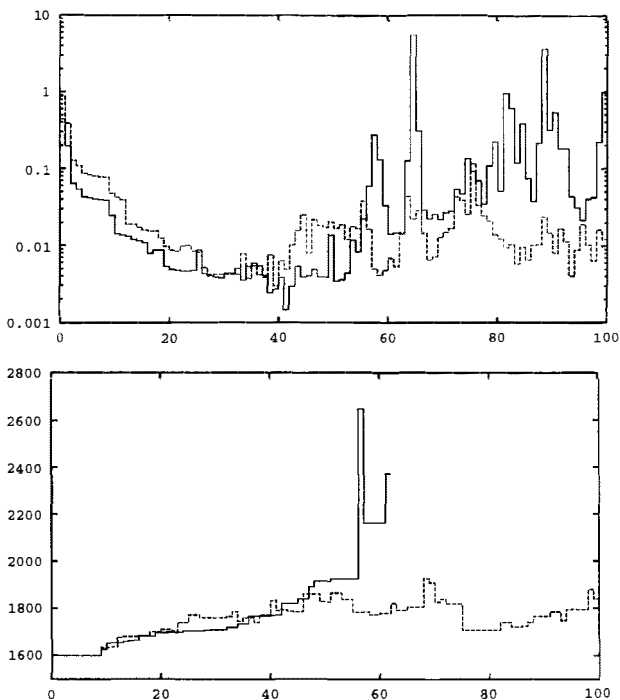


Figure 1. Top: evolution of the cost functional as a function of the number of iterations; bottom: corresponding evolution of the scatterer velocity c using the approximated calculation of the derivative with respect to the contrast (—) and the full one (- -).

4. Conclusion

Results shown so far are still provisional. Complementary experiments are needed, with the help of both approximated and full evaluation of the derivatives of the cost functional with respect to the contrast, for more complicated configurations (such as an object confined within a layer of a stratified space or lossy media), but proper retrieval of both shape and contrast with a level set method is certainly promising.

References

1. S. Osher and J. A. Sethian, *J. Comput. Phys.*, **79**, 12–49 (1988).
2. J. A. Sethian, *Levelset Methods and Fast Marching Methods*, Cambridge University Press, 2nd edition (1999).
3. A. Litman, D. Lesselier, and F. Santosa, *Inverse Problems*, **14**, 658–706 (1998).
4. O. Dorn, E. L. Miller, and C. M. Rappaport, *Inverse Problems*, **16**, 1119–1156 (2000).

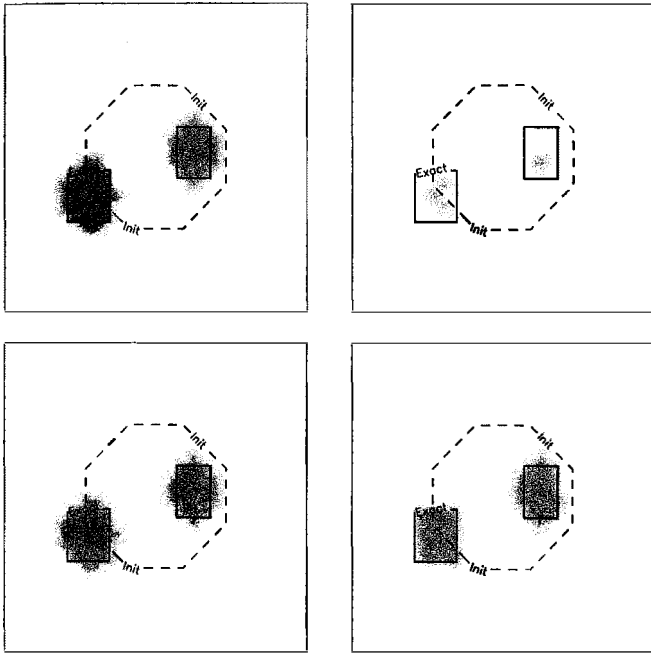


Figure 2. Refer to Fig. 1. Black-and-white representations of the retrieved domains using the approximated calculation of the derivative with respect to the contrast (top row, left at iteration 41, right at iteration 100) and the exact one (bottom row, left at iteration 39, right at iteration 100). The initial contour is displayed as a dashed line.

5. C. Ramananjaona, M. Lambert, D. Lesselier, and J.-P. Zolésio, *Inverse Problems*, **17**, 1087–1111 (2001).
6. H. Feng, D. A. Castañon, and W. C. Karl, *IEEE Trans. Image Process.*, to appear.
7. J. Sokółowski and J.-P. Zolésio, *Introduction to Shape Optimization. Shape Sensitivity Analysis*, Springer Verlag, (1992).
8. R. F. Harrington, *Field Computation by Moment Method*, Macmillan (1968).
9. C. Ramananjaona, *Méthodes d'ensembles de niveaux pour la résolution de problèmes inverses des ondes*, Thèse de Doctorat, Université de Versailles-Saint-Quentin-en-Yvelines (2002).
10. A. Franchois and C. Pichot, *IEEE Trans. Antennas Propagat.*, **45**, 203–215 (1997).
11. M. Cuer and J.-P. Zolésio, *Systems and Control Letters*, **11** 151–158 (1988).
12. D. H. Brandwood, *Proceedings of the IEE-H*, **130** 11–16 (1983).